UPPER CROSS-SECTION LIMIT FOR THE ^{248}Cm(^{50}Ti, xn)$^{298-x}$Og REACTION*

M.W. Bordeau [a,b], B.J.P. Gall [a,b], K. Morita[b,c]
K. Morimoto [b], D. Kaji [b], S. Ishizawa[b,d], T. Niwase [b,c]
S. Yamaki[b,e], H. Haba [b], Y. Komori[b], T. Yokokita[b]
K.P. Rykaczewski [f], K. Kessaci [a,b], Z. Asfari[a,b]
T. Tanaka [a,b,c], P. Brionnet [b], H. Arakawa[e], M. Asai[b,g]
O. Dorvaux [a,b], M. Filliger[a], T. Fujii[e], K. Fujita[b,g], S. Goto[b,h]
E. Ideguchi [b,i], K. Inomata[e], Y. Ito[b,g], H. Kikunaga[b,j]
H. Kudo[b,h], S. Mitsuoka[c], B.C. Rasco [f], H. Sakai [b]
F. Tokanai[b,d], A. Toyoshima[b,k], T. Yamaguchi[b,e]

[a]Université de Strasbourg, CNRS, IPHC UMR 7178, 67037 Strasbourg, France
[b]RIKEN Nishina Center for Accelerator-Based Science
Wako, Saitama 351-0198, Japan
[c]Department of Physics, Kyushu University, Fukuoka 819-0395, Japan
[d]Faculty of Science, Yamagata University, Yamagata 990-8560, Japan
[e]Department of Physics, Saitama University, Saitama 338-8570, Japan
[f]Oak Ridge National Laboratory, Oak Ridge, TN 37831, USA
[g]Advanced Science Research Center, Japan Atomic Energy Agency (JAEA)
Tokai, Ibaraki 319-1195, Japan
[h]Department of Chemistry, Niigata University, Niigata 950-2181, Japan
[i]Research Center for Nuclear Physics (RCNP), Osaka University
Ibaraki Mihogaoka, Osaka 567-0047, Japan
[j]Research Center for Electron Photon Science, Tohoku University
Sendai 980-8578, Japan
[k]Institute for Radiation Sciences, Osaka University, Suita 565-0871, Japan

Received 31 October 2025, accepted 10 February 2026,
published online 31 March 2026

The synthesis of oganesson ($Z = 118$) using a metallic beam was investigated at the RIKEN Nishina Center with the ^{248}Cm(^{50}Ti,xn)$^{298-x}$Og fusion–evaporation reaction, performed on RILAC and GARIS-II separators. This experiment was conducted for 39 days. No Og decays were detected. A total dose of 4.93×10^{18} projectiles was accumulated on the target, reaching a sensitivity of 0.27 pb and an upper cross-section limit of 0.50 pb.

DOI:10.5506/APhysPolBSupp.19.1-A25

* Presented at the XXXVIII Mazurian Lakes Conference on Physics, Piaski, Poland, August 31–September 6, 2025.

1. Introduction

The stability of atomic nuclei originates from the strong nuclear force, which counteracts the Coulomb repulsion between protons up to mass numbers of about $A \leq 150$. For heavier nuclei, additional binding from quantum shell effects is essential. Superheavy elements (SHE), with $Z > 104$, do not exist naturally but have been artificially produced and investigated for their physical and chemical properties (see [1]). Two main synthesis strategies have been developed. First, the cold fusion approach used ^{208}Pb and neighboring isotopes [2] as targets with heavy projectiles, minimizing excitation energy and fission probability. It was pushed up to the production of nihonium ($Z = 113$) via ^{209}Bi(^{70}Zn,n)^{278}Nh, with a cross section of 19^{+19}_{-10} fb [3]. Second, the hot fusion method [4–6] used the neutron-rich doubly magic ^{48}Ca projectile ($Z = 20$) colliding with actinide targets. This technique has reached its practical limits with californium ($Z = 98$), the heaviest target material available in sufficient quantities [7, 8].

The extension of SHE synthesis beyond $Z = 118$ requires intense metallic beams such as ^{50}Ti, ^{51}V, ^{54}Cr, ^{58}Fe, and ^{64}Ni, but the reaction cross sections are predicted to decrease significantly with heavier projectiles ($Z > 21$) [9], making the establishment of reference reactions with known SHE crucial before pursuing new element search. As ^{294}Og is the heaviest nucleus produced yet, it is an ultimate anchor point to estimate the feasibility of new elements with this type of beam [10].

2. Experimental setup

The ^{248}Cm(^{50}Ti,xn)$^{298-x}$Og experiment was performed in RIKEN. The intense ^{50}Ti beam was based on MIVOC organo-metallic compounds prepared by IPHC, Strasbourg [11]. It was accelerated by the RIKEN Linear Accelerator (RILAC) to an energy of 227.9(5) MeV at an average on-target intensity of 0.34 pμA.

The ^{248}Cm was deposited by molecular plating [12] as $Cm(NO_3)_3$ on 2.1(2) μm thick natural titanium backing foils and then placed on a 10 cm diameter target wheel (see Fig. 1). It was mounted in a water-cooled semi-closed inner-target box and was rotated at 1200 rpm [13]. The Cm turned to oxide during the "target cooking" process in the first hours of beam time. The isotopic composition of the target was: ^{248}Cm: 96.646%, ^{247}Cm: 0.040%, ^{246}Cm: 3.167%, ^{245}Cm: 0.130%, and ^{244}Cm: 0.017%. The average thickness of the Cm layer over the 8 sectors was measured to be 444(11) μg/cm^2 (Table 1).

To monitor the ^{50}Ti^{11+} beam intensity and determine the dose accumulated on target, a silicon PIN-photodiode (covering 3.6×3.6 mm^2) was mounted at an angle of 45° with respect to the beam axis, 20.0 cm down-

stream from the target. It covered a solid angle of 0.324 msr, and was partially screened by a 0.5 mm thick aluminum foil gridded with 0.1 mm diameter holes ensuring a 1% transmission, in order to protect the PIN-diode from dose-induced deterioration.

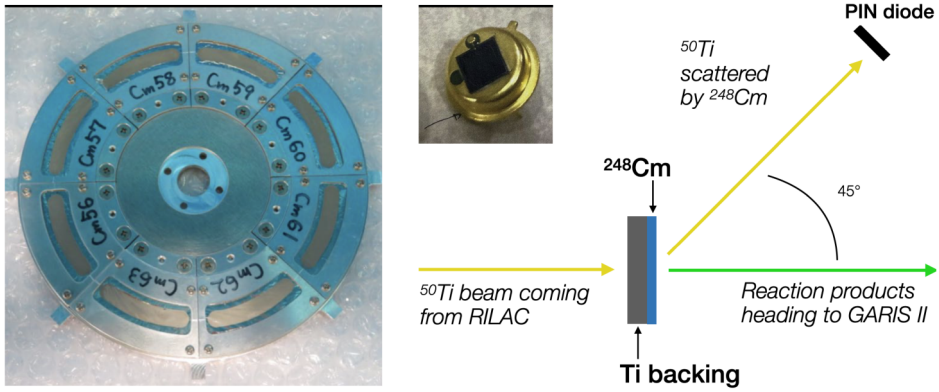

Fig. 1. Left: Photograph of the eight sectors target wheel before irradiation. Top center: Adapted from [10] photograph of the Si PIN diode. Right: Scheme of the Rutherford scattering of ^{50}Ti on ^{248}Cm.

Table 1. Target characteristics: Ti backing thickness, thickness of the ^{248}Cm, energy losses in the backing (ΔE_{Ti}), energy losses in the first half Cm_2O_3 material (ΔE_{Cm}), and the center-of-mass energy in the middle of the Cm target ($E_{1/2_{\mathrm{CoM}}}$).

Target		Ti	^{248}Cm	ΔE_{Ti}	ΔE_{Cm}	$E_{1/2_{\mathrm{CoM}}}$
#	id	[μm]	[μg/cm^2]	[MeV]	[MeV]	[MeV]
1	Cm61	2.069	461.9	13.9	2.2	227.9
2	Cm60	2.069	451.4	13.9	2.2	227.9
3	Cm59	2.091	438.0	14.1	2.1	227.9
4	Cm58	2.091	432.3	14.1	2.1	227.9
5	Cm57	2.052	421.0	13.8	2.0	228.2
6	Cm56	2.052	430.7	13.8	2.1	228.1
7	Cm63	2.095	460.8	14.1	2.2	227.9
8	Cm62	2.095	456.5	14.1	2.2	227.8
Average		2.1(2)	444(11)	14.0	2.1	227.9(6)

GARIS-II (GAs-filled Recoil Ion Separator) is used to separate the reaction products from the beam after the target. Its structure, as shown in Fig. 2, allows for an efficient selection of these nuclei. It was operated with 0.73 mbar of helium gas to equilibrate the charge states of recoiling ions, ensuring a transport efficiency of approximately 75% (for the entire system) [15]. A magnetic rigidity of 2.22 T m was set based on previously measured values [14] for neighboring nuclei.

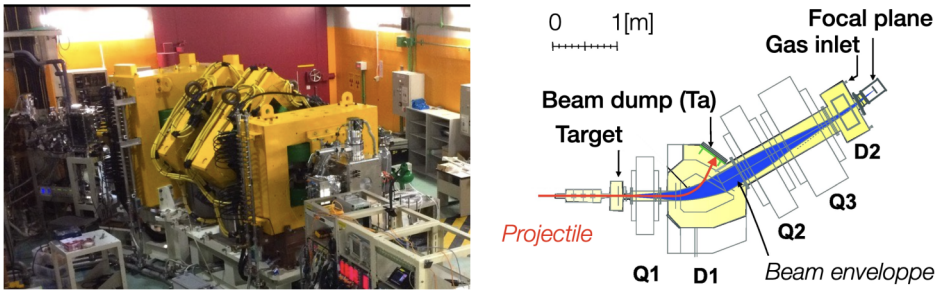

Fig. 2. Left: Photograph of GARIS-II and the focal plane detection setup. Right: Schematic cross section of GARIS-II. (Adapted from [14]).

Exiting the separator through 0.5 μm Mylar foil, the compound nucleus (CN) enters the focal plane detection system (FPDS), see Fig. 3, which is composed of:

- a time-of-flight (TOF) detector with an effective area of 154 cm^2,
- an assembly of 24 PIN-diodes (28 $\times$ 28 mm^2 each) in a tunnel geometry,
- 2 double-sided silicon detectors (DSSD) of 16 $\times$ 16 stripes forming a 100 $\times$ 50 mm^2 implantation area,
- 4 silicon detectors (SSD) placed behind the DSSD as light particles veto.

The DSSD width defines a $\pm$1.5% window in magnetic rigidity. Association of 32 (16 from each side) X–Y strips data enables a pixel analysis with lower background and longer time correlation. Strips on the backside of the DSSD are set on a 10 times lower gain to detect fission products energy, which is one to two orders of magnitude higher than expected α-decays. The FPDS (DSSD+tunnel) ensures an 80% detection efficiency of escaping α particles. Signals from silicon detectors were shaped and their amplitudes extracted by 16-channel MESYTEC MSCF-16-F boards, and fetched to 32-channel ADC MESYTEC MADC-32 boards.

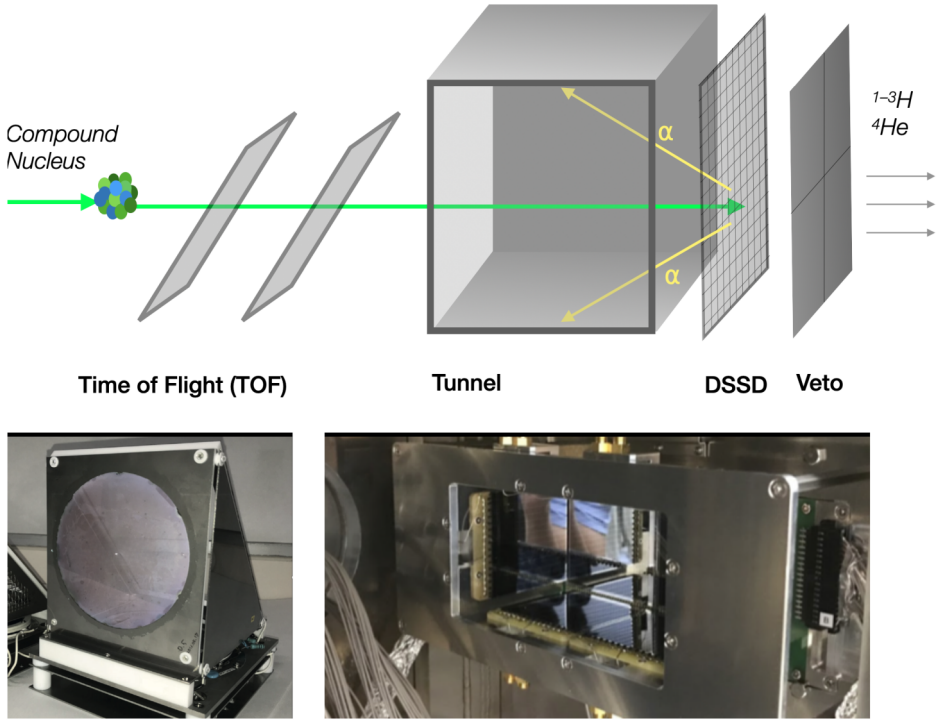

Fig. 3. Top: Scheme of the FPDS. Bottom left: Photograph of the time-of-flight detector. Bottom right: Silicon detector box (Tunnel) and the DSSD where nuclei are stopped. Courtesy of K. Morimoto.

Calibration of the FPDS was done by producing isotopes with well known α-decay energies, using ^{50}Ti beam at energy of 248.3 MeV (lab) on a ^{159}Tb target. These fusion–evaporation reactions are:

— $^{159}\mathrm{Tb}(^{50}\mathrm{Ti}, xn)^{209-x}\mathrm{Fr} - E_\alpha = 6.916$ MeV (^{205}Fr); 7.031 MeV (^{204}Fr),

— $^{159}\mathrm{Tb}(^{50}\mathrm{Ti}, pxn)^{208-x}\mathrm{Ra} - E_\alpha = 7.340$ MeV (^{205}Ra),

— $^{159}\mathrm{Tb}(^{50}\mathrm{Ti}, \alpha xn)^{205-x}\mathrm{At} - E_\alpha = 6.344$ MeV (^{201}At); 6.538 MeV (^{200}At).

At 7 MeV, the α-energy resolution was 35 keV for the DSSD and 120 keV for the tunnel's silicon detectors.

The collision energy for the production of $^{293-294-295}$Og was determined by a Coulomb barrier measurement experiment [16, 17], an excitation function being unreachable due to the very low cross sections. A mid-target energy of 290.0(6) MeV was calculated and set for the experiment.

3. Data analysis

The expected decay chains for $^{293-294-295}$Og are presented in Fig. 4. Previous observations for ^{294}Og and its decay chain allow us to predict the α-decay being in a 10.5–12 MeV energy range, and a lifetime in the order of milliseconds. Several search strategies were used in parallel:

— Implantation in DSSD followed by one α-decay from the Og decay list;
— Implantation in DSSD followed by two α-decays from the Og decay list;
— Three consecutive α-decays from the Og decay list;
— Back-search starting from a spontaneous fission (SF) event and looking for the former content of the strip data;
— Implantation in DSSD followed by an α-decay from the list and an SF;
— Direct search of ^{290,291}Lv;
— Two consecutive α-decays from the list followed by an SF.

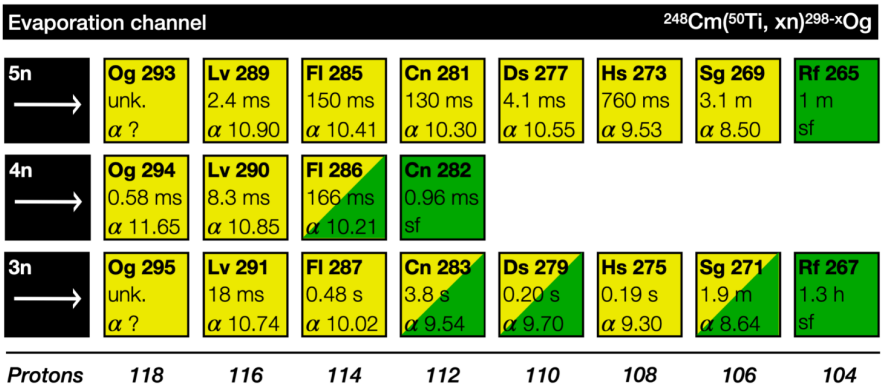

Fig. 4. (Color online) Decay chains corresponding to the 3–5n exit channels. The energies are given in MeV [18].

Despite the various methods used by the independent analysts presented in [10], no decay of Og isotopes was found in the data of the experiment. An upper-limit and a one-event cross section are therefore proposed.

The dose accumulated on target is determined by analysis of elastic scattering (or Rutherford Scattering, RS) from the ^{50}Ti projectiles on the ^{248}Cm target material. The RS data were timestamped by a dedicated clock unit that was reset at each rotation of the target. This allowed us to visualise the RS spectra as a function of the target timestamps to display each individual sector (see Fig. 5). The main peak of the spectrum corresponds to the elastic scattering of ^{50}Ti on ^{248}Cm. A secondary peak corresponds to ^{50}Ti being scattered by a small lanthanide contamination of the Cm.

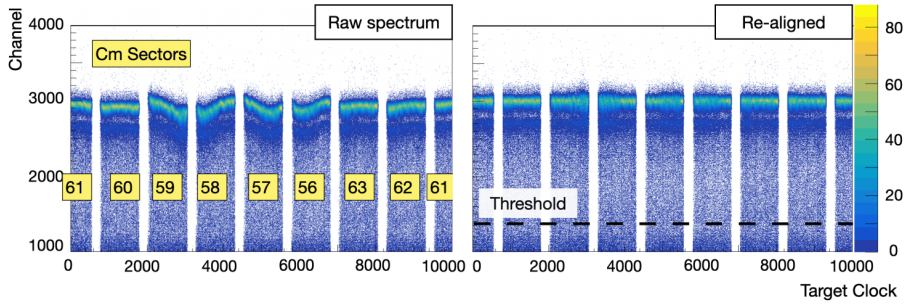

Fig. 5. (Color online) Plot of the Rutherford scattering (RS) energy as a function of the target clock, for both raw and realigned data (arbitrary units). The "yellow line" is the "^{50}Ti scattered by the ^{248}Cm" peak for each sector.

The number of "^{50}Ti scattered by ^{248}Cm" is generally extracted by taking counts in a certain range of energy (uncalibrated). In our case, such a method overestimates the dose due to the lanthanide contamination of the Cm material. The methods applied to remove this contribution and to estimate the total dose can be found in [10]. We determined that about 4.93×10^{18} projectiles reacted with the Cm target, establishing a sensitivity for one event of 0.27 pb, and a 1σ upper cross-section limit of 0.50 pb.

4. Results and discussion

The present experiment achieved an upper limit of 0.50 pb and a one event cross section of 0.27 pb , this last value being comparable to the previously measured cross section of $\sigma = 0.5^{+1.6}_{-0.3}$ pb for oganesson synthesised in ^{48}Ca-induced fusion–evaporation reactions [19, 20].

According to theoretical estimates by Zagrebaev [9], the transition from ^{48}Ca to ^{50}Ti projectiles is expected to reduce the production cross section by approximately one order of magnitude. However, direct comparisons between reactions involving different projectile–target combinations are inherently difficult, as key parameters such as Q-values, fission barriers, and potential energy surfaces are not independently controllable. This emphasizes the importance of obtaining experimental benchmark points. The recent ^{50}Ti-induced production cross section of $\sigma = 0.44^{+58}_{-28}$ pb for ^{290}Lv ($Z = 116$) from Berkeley [21] is one order of magnitude lower than the ^{48}Ca-induced 4n-channel cross sections reported by Dubna ($3.3^{+2.5}_{-1.4}$ pb) [22], GSI ($3.4^{+2.7}_{-1.6}$ pb) [23], and RIKEN ($3.1^{+2.8}_{-1.8}$ pb) [24], which confirms experimentally Zagrebaev's prediction.

Consequently, a sensitivity of approximately 50 fb would be required to detect a single oganesson nucleus produced via the ^{50}Ti + ^{248}Cm reaction. This would correspond to a total integrated beam dose of about 2.7×10^{19} projectiles on a Cm target similar to that used in the present work. At an average beam intensity of 1 pμA, this sensitivity could be achieved in roughly 50 days with current facilities. This achievement would provide a key experimental reference point at the upper edge of the nuclear chart, that will trig improvement of theoretical modeling of fusion–evaporation cross sections for future SHE experiments.

REFERENCES

[1] Ch.E. Düllmann, R.-D. Herzberg, W. Nazarewicz, Y. Oganessian, *Nucl. Phys. A* **944**, 1 (2015).
[2] S. Hofmann, G. Münzenberg, *Rev. Mod. Phys.* **72**, 733 (2000).
[3] K. Morita, *Nucl. Phys. A* **944**, 30 (2015).
[4] Yu.Ts. Oganesian *et al.*, *JETP Lett.* **20**, 265 (1974).
[5] Yu.Ts. Oganessian, «Fusion and fission induced by heavy ions», in: «Classical and Quantum Mechanical Aspects of Heavy Ion Collisions», *Springer Berlin Heidelberg*, Berlin, Heidelberg 1975.
[6] G.N. Flerov *et al.*, *Nucl. Phys. A* **267**, 359 (1976).
[7] J.B. Roberto *et al.*, *Nucl. Phys. A* **944**, 99 (2015).
[8] N.T. Brewer *et al.*, *Phys. Rev. C* **98**, 024317 (2018).
[9] V. Zagrebaev, W. Greiner, *Phys. Rev. C* **78**, 034610 (2008).
[10] B.J.P. Gall *et al.*, *J. Phys. Soc. Jpn.* **94**, 094201 (2025).
[11] J. Rubert *et al.*, *Nucl. Instrum. Methods Phys. Res. B* **276**, 33 (2012).
[12] H. Sakai, H. Haba, K. Morimoto, N. Sakamoto, *Eur. Phys. J. A* **58**, 238 (2022).
[13] D. Kaji, K. Morimoto, *Nucl. Instrum. Methods Phys. Res. A* **792**, 11 (2015).
[14] D. Kaji, K. Morita, K. Haba, H. Kudo, *Proc. Radiochim.* **1**, 105 (2011).
[15] D. Kaji *et al.*, *RIKEN Accel. Prog. Rep.* **47**, 41 (2014), https://www.nishina.riken.jp/researcher/APR/APR047/pdf/41.pdf
[16] T. Tanaka *et al.*, *J. Phys. Soc. Jpn.* **87**, 014201 (2018).
[17] T. Tanaka *et al.*, *Phys. Rev. Lett.* **124**, 052502 (2020).
[18] Z. Sóti, J. Magill, R. Dreher, *EPJ Nuclear Sci. Technol.* **5**, 6 (2019).
[19] Yu.Ts. Oganessian *et al.*, *Phys. Rev. Lett.* **109**, 162501 (2012).
[20] Yu.Ts. Oganessian *et al.*, *Phys. Rev. C* **74**, 044602 (2006).
[21] J.M. Gates *et al.*, *Phys. Rev. Lett.* **133**, 172502 (2024).
[22] Yu.Ts. Oganessian *et al.*, *Phys. Rev. C* **70**, 064609 (2004).
[23] S. Hofmann, *Eur. Phys. J. A* **48**, 62 (2012).
[24] D. Kaji *et al.*, *J. Phys. Soc. Jpn.* **86**, 034201 (2017).